Application of X-ray Absorption Spectroscopy in Determining the Crystal Structure of Low-Dimensional Compounds. Iron Oxychloride and Its Alkoxy Substituents

Jin-Ho Choy,* Joo-Byoung Yoon, Dong-Kuk Kim, and Sung-Ho Hwang

Department of Chemistry, College of Natural Sciences, Seoul National University, Seoul 151-742, Korea

Received June 15, 1995[⊗]

X-ray absorption spectroscopic studies at the Fe K-edge have been performed for iron oxychloride, FeOCl, and its alkoxy substituents, $FeOCl_{1-x}(OR)_x$, where R is CH_3 or C_2H_5. By comparison with the X-ray absorption near edge structure (XANES) spectra for some references such as γ-FeOOH, Fe_3O_4, and $Fe(acac)_3$, it was confirmed that the iron octahedra become regular as the amount of substitution increases, even though the valence state of the iron remains unchanged by substitution reaction. Detailed information on crystal structure, including bond angles as well as bond distances, was obtained from multiple scattering extended X-ray absorption fine structure (EXAFS) analyses of FeOCl and its methoxy substituent over long range up to ~6 Å. We utilized a minimal set of adjustable parameters (only five interatomic distances and the associated ΔE_0, and Debye−Waller factors), letting geometry do the rest of the work for them. The resultant structure for the methoxy substituent showed that the local symmetry around the iron becomes higher than that for FeOCl and also is very similar to that for γ-FeOOH as expected from the XANES spectra. One-dimensional electron-density map along the *c*-axis was obtained in two different ways; one was from X-ray diffraction intensities and the other from EXAFS fitting results. The two one-dimensional electron-density maps were in good agreement, which reflects the reliability of the EXAFS fit. This EXAFS analytical method could be effectively applied to various two-dimensional systems with very poor crystallinity.

Introduction

Much research has been carried out on the preparation of new intercalation complexes of transition metal oxychlorides (MOCl, where M = Ti, V, Cr, and Fe) with unusual physicochemical properties.[1−3] Some attempts were also made to explore new layered compounds through the topochemical substitution of chlorine layers in MOCl with ammonia, alkylamine, and alcohol, leading to the formation of MONHR,[4,5] $MO(OCH_3)$,[6,7] and $MO(O_2C_2H_4)_{1/2}$,[8] respectively. Thereafter, it was reported that *n*-alkanol intercalation complexes of $FeOCl(C_nH_{2n+1}OH)_{0.5}$ ($n \approx 1-18$) could be condensed to $FeOCl_{0.5}(OC_nH_{2n+1})_{0.5}$, which were also capable of forming intercalation complexes.[9] More recently, three kinds of topochemical substituents of FeOCl have been studied to show good cathode performance in the rechargeable lithium batteries.[10]

From a synthetic chemistry point of view, the surface modification of MOCl by intercalating organic molecules or substituting them for chlorine atoms would be a potential way of preparing various new two-dimensional organic derivatives of MOCl, and their detailed crystal structures are a prerequisite for understanding the physical and chemical properties. However, it is very difficult to obtain single crystals of such organic derivatives since they are easily broken into fine powder because of the considerable elastic deformation during the intercalation or substitution reactions. Therefore, many such studies have been performed under the assumption that their two-dimensional lattice structure may be unchanged by intercalation or substitution, but this can lead to incorrect interpretations of various physicochemical properties. This is probably the reason why only a few studies have been performed on these systems in the last decade.

In this regard, X-ray absorption spectroscopy (XAS) is a useful tool for determining the structure of such materials since it is very sensitive to the local environment around specific atoms, irrespective of crystallinity or dimensionality of solids; this can also allow us to estimate the number and the type of atoms around the central absorbing atom and to determine accurately the interatomic distances.[11−13] Generally, extended

* To whom all correspondence should be addressed: Fax, 82-2-872-9864; telephone, 82-2-880-6658; e-mail, jhchoy@alliant.snu.ac.kr.

⊗ Abstract published in *Advance ACS Abstracts,* November 1, 1995.

(1) (a) Meyer, H.; Weiss, A.; Besenhard, J. O. *Mater. Res. Bull.* **1978**, *12*, 913. (b) Maguire, J. A.; Banewicz, J. J. *Mater. Res. Bull.* **1984**, *19*, 1573.

(2) (a) Halbert, T. R.; Scanlon, J. *Mater. Res. Bull.* **1979**, *14*, 415. (b) Schafer-Shahl, H.; Abele, R. *Angew. Chem. ,Int. Ed. Engl.* **1980**, *19*, 477. (c) Halbert, T. R.; Johnston, D. C.; McCandish, L. E.; Thompson, A. H.; Scanlon, J. C. *Physica B* **1980**, *99*, 128.

(3) (a) Kanamura, F.; Koizumi, M. *Jpn. J. Appl. Phys.* **1974**, *13*, 1319. Herber, R. H.; Maeda, Y. *Inorg. Chem.* **1981**, *20*, 1409. (b) Averill, B. A.; Kauzlarich, S. M. *Mol. Cryst. Liq. Cryst.* **1984**, *107*, 55. (c) Choy, J. H.; Uh, J. W.; Kang, J. K.; Weiss, A.; Rey-Lafon, M. *J. Solid State Chem.* **1987**, *77*, 60. (d) Pieczko, M. E.; Breen, J. J. *Langmuir* **1995**, *11*, 1412.

(4) (a) Hagenmuller, P.; Rouxel, J.; Portier, J. *C. R. Acad. Sci.* **1962**, 2000. (b) Hagenmuller, P.; Rouxel, J.; Buckier, P. *Z. Anorg. Allg. Chem.* **1967**, *355*, 209. (c) Weiss, A.; Choy, J. H. *Z. Naturforsch.* **1984**, *39B*, 1193.

(5) (a) Choy, J. H.; Weiss, A. *Diskussionsvortrag, 17*; Hauptversammlung der GDCh: München, Germany, 1977. (b) Choy, J. H. Ph.D. Dissertation, Universität München, München, Germany, 1979.

(6) Kikkawa, S.; Kanamura, F.; Koizumi, M. *Inorg. Chem.* **1976**, *15*, 2195.

(7) (a) Choy, J. H.; Kang, J. K.; Kwon, Y. U. *Bull. Korean Chem. Soc.* **1985**, *6*, 251. (b) Rouxel, J.; Palvadeau, P.; Venien, J. P.; Villieras, J.; Janvier, P.; Bujoli, B. *Mater. Res. Bull.* **1987**, *22*, 1217.

(8) Son, S.; Kikkawa, S.; Kanamura, F.; Koizumi, M. *Inorg. Chem.* **1980**, *19*, 262.

(9) Weiss, A.; Choy, J. H. *Z. Naturforsch.* **1980**, *35B*, 157.

(10) Takehara, Z.; Sakaebe, H.; Kanamura, K. *J. Power Sources* **1993**, *43−44*, 627.

(11) Teo, B. K. In *EXAFS: Basic Principles and Data Analysis*; Springer-Verlag: Berlin, 1986.

(12) Sayers, D. E.; Bunker, B. A. In *X-ray Absorption: Principles, Applications, Techniques of EXAFS, SEXAFS, and XANES*; Koningsberger, D. C., Prins, R., Eds.; Wiley-Interscience: New York, 1988; pp 211−253.

(13) Lytle, F. W. In *Applications of Synchrotron Radiation*; Winick, H., et al., Eds.; Gordon and Breach Science: New York, 1989; pp 135−223.

0020-1669/95/1334-6524$09.00/0

Table 1. Chemical Analyses Results in Weight Percentage for FeOCl and Its Alkoxy Substituents

compounds	Fe	O	Cl	C	H	x^a	y^a	z^a
FeOCl	51.95	14.60	33.45			1.00		
	(52.05)	(14.91)	(33.04)					
methoxy-	51.18	31.52	5.09	9.51	2.70	0.13	0.87	
	(52.44)	(29.97)	(5.22)	(9.75)	(2.44)			
ethoxy-	50.54	21.58	13.01	11.89	2.98	0.40	0.45	0.15
	(51.17)	(21.30)	(13.16)	(12.03)	(2.08)			

[a] $x + y + z = 1$ for the formula, $FeOCl_x(OR)_y(OH)_z$. [b] Values in parentheses are calculated ones.

X-ray absorption fine structure (EXAFS) analysis gives average interatomic distances with an accuracy of ±0.02 Å and gives the type and number of nearest-neighboring atoms up to distances of about 4 Å around a central atom. The most popular technique in EXAFS data analysis is the Fourier-filtering method that isolates the fine-structure due to a single neighboring pair using adequate windows.[12] However, the oscillations of each pair above second neighbors overlap severely in most condensed matter so that it is difficult to determine their crystal structure at higher R ranges using the Fourier-filtering method. Therefore, in order to obtain exact information on the structure by means of EXAFS analysis at higher R ranges, it is important to choose the proper scattering paths and to limit the number of variables through correlation between variables with physical meaning. With this point of view, a new fitting scheme is required to obtain physically meaningful results.

In the present work, we report the detailed structural changes around the iron atoms in FeOCl and its alkoxy substituents using Fe K-edge XAS and show how the crystal structure of low-dimensional compounds up to distances of 6 Å could be determined by the EXAFS method in combination with powder X-ray diffraction.

Experimental Section

Sample Preparations. Iron(III) oxychloride has been prepared from α-Fe_2O_3 (99.98%, Aldrich) and $FeCl_3$ (97%, Aldrich) with a mole ratio of 1:1.3 in a sealed Pyrex tube by a chemical vapor transport technique.[14] Dark-brownish thin plate crystals were obtained after reaction at 370 °C for a week. Since FeOCl is rather sensitive to humidity, the product was dried in vacuum after removing the excess $FeCl_3$ by washing with water-free methanol. The single phase FeOCl was confirmed by powder X-ray diffraction (XRD) analysis. The synthetic γ-FeOOH, as a reference for the XAS experiment, has been prepared from $FeCl_2 \cdot 4H_2O$ (99%, Merck) and NaOH by a previously suggested synthetic method;[15] the powder XRD pattern of the product was in good agreement with the literature. Chemical reagents of Fe(acetylacetonate)$_3$ (99%, Aldrich; acetylacetonate = acac) and Fe_3O_4 (98%, Aldrich) were also used as references for the XAS experiment.

For the preparation of $FeOCl_{1-x}(OC_nH_{2n+1})_x$ (n = 1, 2), methoxide and ethoxide solutions were prepared by adding 0.145 g of fresh cut sodium pieces into 20 mL of the corresponding alcohol dried by a 4A-type molecular sieve. A 500 mg sample of FeOCl below 200 mesh was added to an alkoxide solution in a mole ratio of 1:1.3 under a dried nitrogen atmosphere.[6,7] Then the sealed ampoules were incubated at 80 °C for a week. In the powder X-ray diffraction patterns, the (00l) reflections for the reaction products shift to a lower angle than those for the pristine FeOCl, and the (200) peak of NaCl was also observed at $2\theta = 31.7°$. To remove this byproduct, NaCl, the products were thoroughly washed with water-free methanol and then dried in vacuum.

X-ray Diffraction Analyses. X-ray diffraction patterns were collected at room temperature by a Philips PW3710 based powder diffractometer using Cu $K\alpha$ radiation ($\lambda_{\alpha 1}$ = 1.540 56 Å) operated at 30 mA and 50 kV. The scattering intensities were measured over an angular range of $5° < 2\theta < 80°$ for all samples with a step size of $\Delta(2\theta) = 0.02°$ and a count time of 4.5 s per step. Intensities and positions of the peaks were determined by using the *APD1700* software. The interlayer distance for each compound was averaged by the (00l) reflections. One-dimensional electron-density maps for FeOCl and its methoxy substituent, $FeOCl_{1-x}(OCH_3)_x$, were obtained using seven (00l) reflections along the c-axis. The electron densities, $\rho(z)$, could be constructed by adding the individual function $F_l[(\sin \pi dz)/\pi dz]$ at points $z = l/d$ ($l \approx 0-7$). The magnitudes of the structure factors, $|F_l|$, were the square root of the corrected intensities (I/L_p), where I and L_p are the observed intensity and the Lorentz-polarization factor, $[(1 + \cos^2 2\theta)/(\sin^2 \theta \cos\theta)]$, respectively. Their signs were determined by the fractional positions of Fe, Cl, and O atoms obtained from EXAFS analysis and by their scattering factors taken from the *International Tables for X-Ray Crystallography*.[16]

Elemental Analyses. Elemental analyses for C, H, and N were performed, and the inductively coupled plasma (ICP) method and the Volhard titration were respectively employed to determine the amounts of Fe and Cl (Table 1).

X-ray Absorption Measurements. X-ray absorption measurements were carried out with synchrotron radiation by using the EXAFS facilities installed at beam line 10B of the Photon Factory, the National Laboratory for High Energy Physics (Tsukuba, Japan), operated at 2.5 GeV with about 260−370 mA of stored current. Samples were ground to a fine powder in a mortar and then spread uniformly onto an adhesive tape, which was folded into a few layers to obtain an optimum absorption jump ($\Delta\mu t \approx 1$), enough to be free from thickness and pinhole effects.[17,18] All the data were recorded in transmission mode at room temperature, using a Si(311) channel-cut monochromator. Intensities of the incident and transmitted beams were measured in N_2- and 25% Ar−75% N_2-filled ionization chambers, respectively. To ensure spectral reliability, much care was taken to evaluate the stability of the energy scale by monitoring the spectra of Fe metal for each measurement, and thus, edge positions were reproducible to better than 0.05 eV.

XANES and EXAFS Data Analyses. The data analyses for experimental spectra were performed by a standard procedure as follows.[11-13] The inherent background in the data was removed by fitting a polynomial to the pre-edge region and then extrapolated through the entire spectrum from which it was subtracted. The resulting spectra, $\mu(E)$, were normalized to an edge jump of unity for comparing the X-ray absorption near edge structure (XANES) features directly to one another. The absorption spectrum for the isolated atom, $\mu_0(E)$, was approximated by a cubic spline. The EXAFS function, $\chi(E)$, was obtained as $\chi(E) = \{\mu(E) - \mu_0(E)\}/\mu_0(E)$.

Further analysis was performed in both k and R spaces, where the photoelectron wave vector k is defined as $k = \{(8\pi^2 m/h^2)(E - E_0)\}^{1/2}$, where m is the electron mass and E_0 is the threshold energy determined as 7121 eV at half-height of the absorption edge jump. The resulting EXAFS spectra were k^3-weighted in order to compensate for the attenuation of EXAFS amplitude at high k and then Fourier transformed in the range ~ 2.5 Å$^{-1} \leq k \leq \sim 14$ Å^{-1} with a Hanning apodization function of $dk = 0.5$ Å^{-1}.

In order to determine the structural parameters, a nonlinear least-squares curve fitting was performed in the region of $R \leq 6$ Å corresponding to the distance to the next nearest Fe along the b-axis in

(14) Halbert, M. R. In *Intercalation Chemistry*; Whittingham, M. S., Jacobson, A. J., Eds.; Academic Press: New York, 1982; pp 375−403.
(15) Naono, H.; Nakai, K. *J. Colloid Interface Sci.* **1989**, *128*, 146.
(16) (a) In *International Tables for X-Ray Crystallography*; Kynoch: Birmingham, U.K., 1974; Vol IV. (b) Adams, J. M. *J. Chem. Soc., Dalton Trans.* **1974**, 2286. (c) Katsaras, J. *J. Phys. Chem.* **1995**, *99*, 4141.
(17) Lytle, F. W.; van der Laan, G.; Greegor, R. B.; Larson, E. M.; Violet, C. E.; Wong, J. *Phys. Rev. B* **1990**, *41*, 8955.
(18) Stern, E. A.; Kim, K. *Phys. Rev. B* **1981**, *23*, 3781.

Table 2. Fitted Structural Parameters for FeOCl[d]

atom	C.N.[a]	R (Å)[b]	σ^2 ($\times 10^{-3}$/Å^2)[b]	ΔE_0 (eV)	crystallographic distance (Å)[a]
O(1)	2	1.96	2.5	−1.2	1.964
O(2)	2	2.12	18.2	−0.9	2.100
Cl(1)	2	2.36	9.2	0.6	2.368
Fe(1)	4	3.10	7.8	−3.6	3.107
Fe(b)	2	3.32	5.5	−3.6	3.302
Fe(a)	2	3.81	4.8	−3.6	3.780
Cl(2)	2	3.96	13.5	1.3	4.003
Cl(3)	4	4.48	14.1	5.7	4.460
Fe(2)	4	5.05	9.3	3.8	5.019
Fe(3)	4	5.59	7.9	−2.9	5.608
Fe(4)	4	6.21	10.1	1.2	6.183
Fe−O(1)−Fe(a)	DS	3.86(152.1°)[c]	8.7	−0.1	148°
	TS	3.92(152.1°)[c]	11.4	13.6	148°
Fe−O(1)−Fe(4)	DS	6.26(157°)[c]	12.8	−3.6	157°
Fe−Fe(b)−Fe(5)	TS	6.64(180°)[c]	9.5	−2.1	180°

[a] Coordination number (C.N.) is fixed to the crystallographic value in ref 22. [b] Fitting accuracy is about 0.02 Å for distance and 25% for the Debye Waller factor. [c] In the case of multiple scattering, the bond angles in parentheses are not fitting parameters but are the values calculated from the EXAFS fitting parameter. [d] Fitting reliability,[21] $\Delta\chi^2 = 1310$.

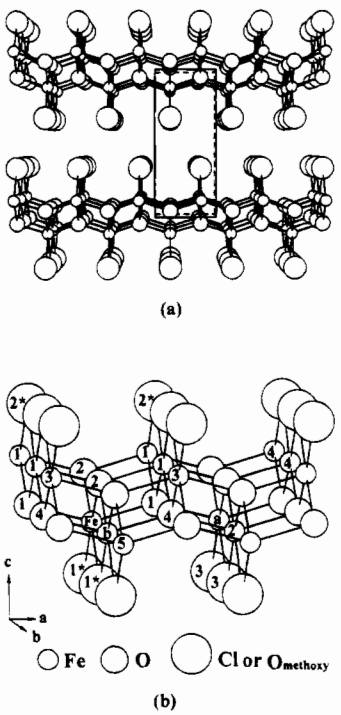

Figure 1. Layer structure of FeOCl: (a) perspective view of the *ac*-plane of the double FeOCl layer where the unit cell is shown by a rectangular box; (b) structural fragments used in EXAFS fitting where the numerical number is attached for the sake of convenience and where * indicates that the Cl(1) and Cl(2) atoms correspond to the $O_{methoxy}(1)$ and $O_{methoxy}(2)$ atoms, respectively, in $FeOCl_{0.13}(OCH_3)_{0.87}$.

the Fourier transform (FT), using the UWXAFS code[19] according to the following EXAFS formula.

$$\chi(k) = -S_0^2 \sum_i \frac{N_i}{kR_i^2} F_i(k) \exp\{-2\sigma_i^2 k^2\} \exp\{-2R_i/\lambda(k)\} \times \sin\{2kR_i + \phi_i(k)\}$$

The backscattering amplitude, $F_i(k)$, the total phase shift, $\phi_i(k)$, and the photoelectron mean free path, $\lambda(k)$, have been theoretically calculated for all scattering paths including multiple scattering ones by a curved wave *ab initio* EXAFS code FEFF5.[20] It should be noted that quantitative EXAFS analysis involving more distant shells beyond the first one becomes very complicated since it needs many adjustable structural parameters and various multiple scattering (MS) paths with single scattering (SS) ones. Therefore, some variables, such as distances (R), the Debye−Waller factor (σ^2), and the threshold energy difference (ΔE_0), should be constrained to reasonable values for the higher shells using structural correlation in crystal geometry. It is also important to properly treat the SS and MS paths contributing to the range of $R \leq 6$ Å. To avoid the unnecessary computations, we need to decrease the number of paths to only those that give significant contributions and to decrease the number of fitting parameters using structural correlation in crystal geometry. The criterion for retaining a path is that the amplitude of the contribution of a given path, when estimated with the plane wave approximation, is above 10% of the first shell maximum peak amplitude. According to the above criterion, a total of 15 paths (11 SS and 4 MS paths) for FeOCl (Table 2) are considered in the fitting procedure.

In the course of EXAFS fitting[21] between the experimental spectrum and the theoretical one, the coordination number (*C.N.*) was fixed to the crystallographic value, and the amplitude reduction factor (S_0^2) was set equal to 0.9[20] for all compounds. In the case of FeOCl, the distances of Fe−O(1), Fe−O(2), Fe−Cl, Fe−Fe(a), and Fe−Fe(b) pair were varied independently, and the others were set to be dependent on these five distances by using a geometrical relation in the unit cell (Figure 1). We also varied σ_i^2 and ΔE_0 for all paths in order to optimize the fit of the theoretical data to the experimental data.

In the case of the methoxy substituent, we calculated the theoretical function by using the FEFF code, assuming the oxygen atoms are completely substituted with chlorine atoms in the unit cell of FeOCl. At first, the outline of the FT spectrum was fitted with 11 SS paths, and then the theoretical functions were recalculated by the FEFF code on the basis of the above results. A total of 12 paths (9 SS and 3 MS paths) were chosen in the final fitting procedure (Table 3).

(19) (a) Newville, M.; Livins, P.; Yacoby, Y.; Rehr, J. J.; Stern, E. A. *Phys. Rev. B* **1993**, *47*, 14126−14131. (b) Frenkel, A.; Stern, E. A.; Voronel, A.; Qian, M.; Newville, M. *Phys. Rev. B* **1994**, *49*, 11662.

(20) (a) Rehr, J. J.; Mustre de Leon, J.; Zabinsky, S. I.; Albers, R. C. *J. Am. Chem. Soc.* **1991**, *113*, 5135. (b) Mustre de Leon, J.; Rehr, J. J.; Zabinsky, S. I. *Phys. Rev. B* **1991**, *44*, 4146. (c) O'Day, P. A.; Rehr, J. J.; Zabinsky, S. I.; Brown, G. E., Jr. *J. Am. Chem. Soc.* **1994**, *116*, 2938.

(21) Fitting reliability is defined as

$$\Delta\chi^2 = \frac{N}{n}\sum_{i=1}^{n}\left\{\frac{\chi_{data}(R_i) - \chi_{theory}(R_i)}{\delta_i}\right\}^2$$

where N is the number of independent data points, $\chi(R_i)$ is the Fourier transform of $\chi(k)$ at the point R_i, n is the number of points used to evaluate $\chi(R_i)$ over the range ΔR, and δ_i^2 is the sum of squares of the measurement uncertainty in $\chi_{data}(R_i)$ and the systematic uncertainties (see also ref 20).

Table 3. Fitted Structural Parameters for $FeOCl_{0.13}(OCH_3)_{0.8}$[d]

atom	C.N.[a]	R (Å)[b]	$\sigma^2(\times10^{-3}/Å^2)$[b]	ΔE_0 (eV)
O(1)	2	2.00	2.7	−1.7
O(2)	2	2.06	3.1	−2.7
$O_{methoxy}(1)$	1.74	1.93	2.5	−3.1
Cl(1)	0.26	2.41	8.3	1.5
Fe(1,*b*)	6	3.09	6.0	0.0
$O_{methoxy}(2)$	2	3.57	4.0	−2.7
O(4)	4	3.68	5.9	−2.7
Fe(*a*)	2	3.89	12.4	0.0
Fe(2)	4	4.97	11.3	0.0
Fe(3)	4	5.35	11.5	0.0
Fe−O(1)−Fe(*a*)	DS	3.94(154.3°)[c]	8.4	−3.7
	TS	3.99(154.3°)[c]	13.6	−11.8
Fe−Fe(*b*)−Fe(5)	TS	6.18(180°)[c]	7.7	−2.1

[a] Coordination number (C.N.) is fixed to the crystallographic value in ref 22. [b] Fitting accuracy is about 0.02 Å for distance and 25% for the Debye Waller factor. [c] In the case of multiple scattering, the bond angles in parentheses are not fitting parameters but are the values calculated from the EXAFS fitting parameter. [d] Fitting reliability,[21] $\Delta\chi^2 = 1101$.

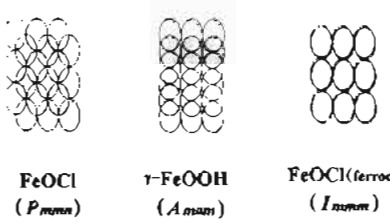

Figure 2. Comparison of interlayer anion packing in FeOX (X = Cl or OH), where the open circles represent the top anions of the lower layer and the hatched circles are the bottom anions of the upper layer. The space groups are indicated and depend on the packing types of the interlayers.

Results and Discussion

Structural Aspect. FeOCl has a layered structure similar to γ-FeOOH and belongs to the orthorhombic space group of *Pmmn* (59) with unit cell dimensions of $a = 3.780$ Å, $b = 3.302$ Å, $c = 7.917$ Å, and $Z = 2$ (Figure 1a).[22] The crystal structures of FeOX, where X is Cl or OH, are generally classified into three types according to an interlayer packing fashion as shown in Figure 2. Although the intralayer network of metal−oxygen in FeOCl is the same type as that in FeOCl−ferrocene and FeOCl−TTF (TTF = tetrathiafulvalene) intercalates (space group of *Immm*)[2,23] or γ-FeOOH (space group of *Amam*),[24] their layers are packed in a rather different way. That is, alternate layers of the FeOX structure in the ferrocene intercalates and γ-FeOOH shift by one-half unit cell along the (110) and (010) directions of FeOCl, respectively. The crystal structure of FeOCl consists of stacks of double sheets of edge-shared *cis*-FeO_4Cl_2 distorted octahedra so that chlorine atoms on the outside of adjacent layers are closely packed in FeOCl. Since the outermost chlorine atoms are weakly bound to strongly interconnected Fe−O layers, it would be possible to replace chlorine by an alkoxy group via the topochemical substitution reaction. As shown in Figure 1a, all the iron atoms are crystallographically equivalent in a unit cell, and the Fe···Fe(*a*) and Fe···Fe(*b*) distances in Figure 1b correspond to unit cell parameters along the *a*- and *b*-axis, respectively.

On the other hand, it was previously reported that the methoxy substituent has a unit cell dimension of $a = 3.83$ Å, $b = 3.99$ Å, and $c = 9.97$ Å from powder X-ray diffraction analysis,[6]

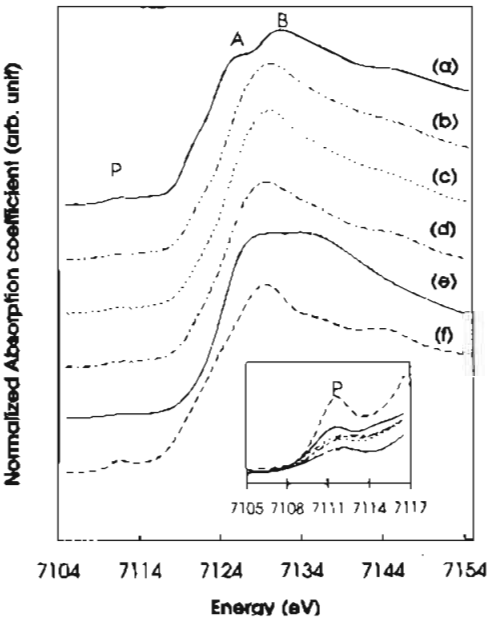

Figure 3. Normalized Fe K-edge XANES spectra of (a) FeOCl, (b) $FeOCl_{0.40}(OC_2H_5)_{0.45}(OH)_{0.15}$, (c) $FeOCl_{0.13}(OCH_3)_{0.87}$, (d) γ-FeOOH, (e) $Fe(acac)_3$, and (f) Fe_3O_4. The inset shows the enlarged-scale view of the pre-edge feature (P), where the pre-edge feature of Fe_3O_4 with the spinel structure is included in order to show that Fe is stabilized in the lower symmetry sites ($T_d + O_h$).

and it was qualitatively suggested that its crystal structure is probably related to that of γ-FeOOH on the basis of powder X-ray diffraction and Mössbauer spectroscopic studies.[6] However, the increment of the *b*-axis is surprisingly too large as pointed out by Halbert.[14] Furthermore, the comparison of its cell parameters to those of γ-FeOOH ($a = 3.87$ Å, $b = 3.06$ Å, and $c = 12.51$ Å)[24] gives rise to some questions about its crystal structure.

Chemical Analyses. The exact formula for methoxy and ethoxy substituents could be determined as $FeOCl_{0.13}(OCH_3)_{0.87}$ and $FeOCl_{0.40}(OC_2H_5)_{0.45}(OH)_{0.15}$, respectively, on the basis of chemical analyses as shown in Table 1. The chlorine is partially substituted by alkoxide since the area demand for an *n*-alkyl chain (cross-sectional area of 4.18 × 4.56 Å^2) is larger than the unit cell area (*ab* plane area of 3.78 × 3.30 Å^2) of FeOCl. Therefore, a complete substitution may be impossible. Similar results could be observed in the intercalation complexes of *n*-alkanol[9] and *n*-alkylamine[3c,4c] in which the change in basal spacing is related to the variation of the packing density of an alkyl chain, and the maximum ratio of organic moieties vs FeOCl was determined to be 0.54 at 22 °C and 0.45 at 110 °C.

Powder X-ray Diffraction. The powder X-ray diffraction patterns for FeOCl and the methoxy- and ethoxy-substituted phases exhibited basal spacings of 7.92, 10.00, and 11.95 Å, respectively, which are dependent upon the size of the alkoxy group as expected. However, it is very difficult to determine exact *a*- and *b*-axis cell parameters for alkoxy substituents because there are only a few non-(00*l*) reflections.

Fe K-Edge XANES Spectroscopy. XANES spectroscopy gives information on the local structure and the electronic state of the absorbing atom. Figure 3 shows the Fe K-edge XANES spectra for FeOCl and its alkoxy substituents, together with γ-FeOOH, $Fe(acac)_3$, and Fe_3O_4 as reference compounds. Although the overall spectral positions are very similar except for Fe_3O_4, reflecting the presence of trivalent iron in all compounds, the detailed spectral features are found to be quite different. In all spectra, a small pre-edge peak denoted as P at ~7112 eV was observed, which has been generally assigned to

(22) Lind, M. D. *Acta Crystallogr. Sect. B* **1970**, *26*, 1058.
(23) Kauzlarich, S. M.; Teo, B. K.; Averill, B. A. *Inorg. Chem.* **1986**, *25*, 1209.
(24) Ewing, F. J. *J. Chem. Phys.* **1935**, *3*, 420.

the 1s → 3d dipolar forbidden transition. According to previous XANES studies[25,26] and molecular orbital calculations[27] on ferric model compounds, this peak gains its intensity from a direct quadrupole coupling to the electromagnetic radiation or a mixing of the 3d and 4p orbitals caused by the breakdown of inversion symmetry due to structural distortion. Consequently, as the local symmetry around the iron is lowered from octahedral symmetry to tetrahedral symmetry, the intensity (I) of this peak tends to increase, i.e., $I_{\text{tetrahedral}} > I_{\text{square pyramidal}} > I_{\text{octahedral}}$. In the inset of Figure 3, we could clearly see the symmetry effect with respect to this peak. Fe_3O_4, with an inverse spinel structure, shows the largest intensity, whereas $Fe(acac)_3$ with regular octahedral symmetry shows the smallest one. In the case of alkoxy substituents, the peak intensity is weaker than that of FeOCl with a highly distorted octahedra but similar to that of γ-FeOOH, implying that the local structure around the iron is modified to a more regular octahedron upon substitution. Such a local structural change upon substitution becomes more prominent at the main peaks denoted as A and B, which are attributed to the dipole-allowed transitions from the 1s core level to the p_π-polarized and the p_σ-polarized 4p orbitals, respectively.[26] The Fe K-edge XANES spectrum for FeOCl clearly exhibits the splitting of the main 1s → 4p transition into A and B, but there is only one peak for the spectra of γ-FeOOH and $Fe(acac)_3$, which has nearly regular octahedral symmetry on the iron site. Similar phenomena are also observed for the spectra of alkoxy substituents, which indicates that the local structure around the iron becomes more symmetric upon the topochemical substitution reaction. According to the present Fe K-edge XANES study, it is clear that the oxidation state (III) of the iron is unchanged by the substitution reaction, and the local structures around the iron in alkoxy substituents become similar to that of γ-FeOOH.

Fe K-Edge EXAFS Spectroscopy. As described before, we believe that EXAFS spectroscopy is the most powerful tool to extend the chemistry of intercalation and substitution (and/or intercalative substitution) of MOCl since the organic derivatives are generally so poor in crystallinity that diffraction or other techniques such as atomic force microscopy (AFM),[3d] could not solve their crystal structure quantitatively. In this study, the local structures of alkoxy substituents were, for the first time, probed by analyzing the EXAFS spectra.

The Fe K-edge k^3-weighted EXAFS spectra for FeOCl, $FeOCl_{0.13}(OCH_3)_{0.87}$, $FeOCl_{0.40}(OC_2H_5)_{0.45}(OH)_{0.15}$, and γ-FeOOH are shown in Figure 4. It should be noted that the EXAFS spectra for alkoxy substituents are very similar to that for γ-FeOOH in shape but differ from that for FeOCl. EXAFS spectra in the range $\sim 2.5\ \text{Å}^{-1} < k < \sim 14\ \text{Å}^{-1}$ were Fourier transformed as shown in Figure 5, in which each FT for FeOCl and γ-FeOOH is in good agreement with results from previous experiments.[23,28]

In Figure 5a, the peaks at ~1.5 and ~2 Å (non-phase-shift-corrected) can be assigned to contributions of the Fe−O and the Fe−Cl bonding pairs, respectively. The peaks in the FT region of 2.4 Å < R < 3.2 Å originate from the nearest Fe···Fe(1) (crystallographic distance of 3.107 Å) and the Fe···Fe(b) pairs whose distance corresponds to the b-axis parameter

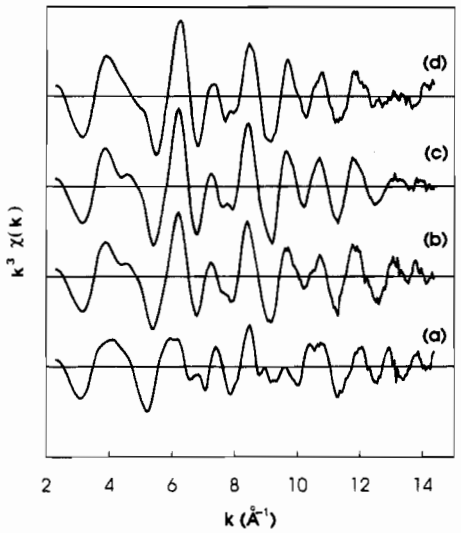

Figure 4. Experimental k^3-weighted Fe K-edge EXAFS spectra of (a) FeOCl, (b) $FeOCl_{0.40}(OC_2H_5)_{0.45}(OH)_{0.15}$, (c) $FeOCl_{0.13}(OCH_3)_{0.87}$, and (d) γ-FeOOH.

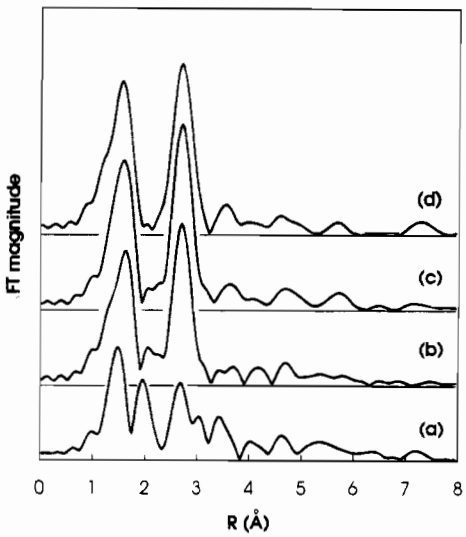

Figure 5. Magnitude of Fourier transforms (non-phase-shift-corrected) of experimental k^3-weighted Fe K-edge EXAFS spectra of (a) FeOCl, (b) $FeOCl_{0.40}(OC_2H_5)_{0.45}(OH)_{0.15}$, (c) $FeOCl_{0.13}(OCH_3)_{0.87}$, and (d) γ-FeOOH shown in Figure 4.

(crystallographic distance of 3.302 Å). On the other hand, the small peaks beyond 3.2 Å could not be assigned simply to contributions of individual scattering paths because various interactions with oxygen, chlorine, and iron atoms overlap severely in this region.

Figure 5 shows clearly that the first-shell peak by the Fe−O interactions gradually increases with the simultaneous decrease of the second-shell peak corresponding to the Fe−Cl interactions as the substitution ratio increases. This result reflects well that the chlorine in FeOCl is substituted with the alkoxy group. On the other hand, because the number of neighboring iron atoms remains unchanged by the topochemical reaction, it could not be readily understood why the third peak for alkoxy substituents increases 3 times larger than that for FeOCl. However, this question could be cleared up through a comparison to the spectra of γ-FeOOH, where the nearest Fe···Fe(1) distance is almost the same as the Fe···Fe(b) distance.[24] Figure 6 shows the EXAFS spectra and their FTs simulated theoretically, assuming that two backscattering iron atoms are located at 3.0 and 3.2 Å, respectively. It is worth noting here that the two EXAFS oscillations interfere destructively with each other. This

(25) (a) Calas, G.; Petiau, J. *Solid State Commun.* **1983**, *48*, 625. (b) Shiro, Y.; Sato, F.; Suzuki, T.; Iizuka, T.; Matsushita, T.; Oyanagi, H. *J. Am. Chem. Soc.* **1990**, *112*, 2921.
(26) Cartier, C.; Momenteau, M.; Dartagy, E.; Fontaine, A.; Tourillon, G.; Michalowicz, A.; Verdaguer, M. *J. Chem. Soc., Dalton Trans.* **1992**, 609.
(27) Roe, A. L.; Schneider, D. J.; Mayer, R. J.; Pyrz, J. W.; Widom, J.; Que, L., Jr. *J. Am. Chem. Soc.* **1984**, *106*, 1676.
(28) Manceau, A.; Conbes, J. M. *Phys. Chem. Miner.* **1988**, *15*, 283.

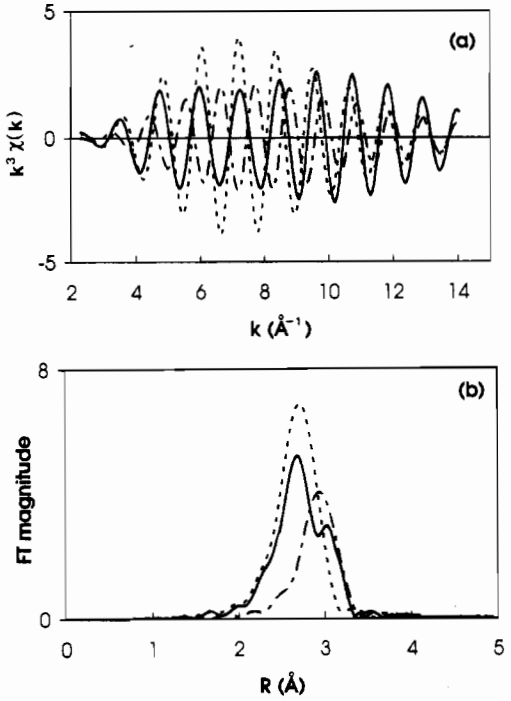

Figure 6. EXAFS oscillations (a) and the corresponding Fourier transforms (b) for Fe−Fe pairs with two different distances of 3.0 Å (- - -) and 3.2 Å (-·-) and their sum (−). Note that two EXAFS oscillations corresponding to individual Fe···Fe distances with a difference of ΔR = 0.2 Å destructively interfere with each other, resulting in a very small magnitude of the FT for FeOCl.

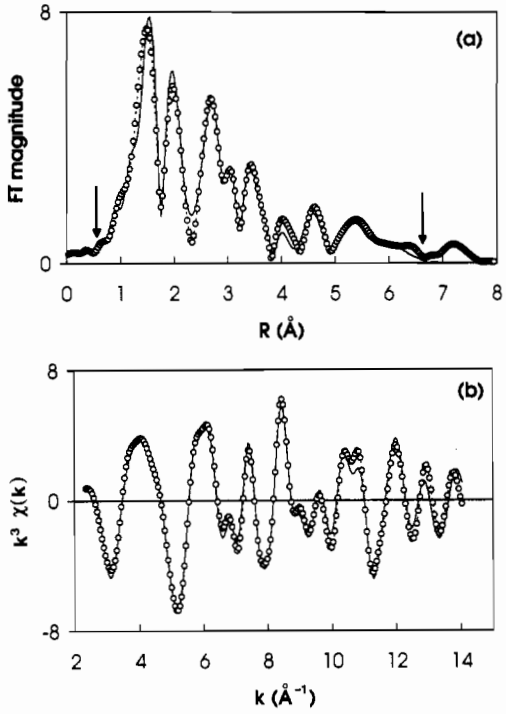

Figure 7. Comparison of the fitted spectra (−) with the experimental data (○) for FeOCl in R (a) and k (b) spaces. The range over which the fit has been made is shown by the arrows.

destructive interference is responsible for the small magnitude of the third-shell peak in FeOCl, while the constructive interference of two oscillations of the Fe···Fe(1) and Fe···Fe-(b) pairs with similar distances induces strong enhancement of the peak in the FT range of about 2.5−3 Å in the case of alkoxy substituents. It should also be noted that such an expectation is inconsistent with the previous powder X-ray diffraction results,[6,8,10] in which the b-axis cell parameter is significantly increased by the substitution reaction.

In order to propose a reasonable structural model for alkoxy substituents, quantitative EXAFS analyses have been performed. At first, the EXAFS spectrum of FeOCl was analyzed on the basis of well-known crystallographic data to confirm the reliability of the curve-fitting method. It should be noted that the peaks in the higher R range of FT are produced by the considerable overlap, which does not, in practice, allow a separation of the contributions by individual paths. Therefore, in order to obtain the correct structural information within this range, all the paths within 6 Å were considered simultaneously during the fitting. As mentioned in the data analyses section, the use of too many variables in the fitting procedure generally tends to give results without any chemical and physical meaning because of strong correlation among structural parameters. Nevertheless, the reason we choose this analytical method is that some geometric constraints between scattering paths could be placed on this system, resulting in the reduction of the number of fitting parameters. Since the FeOCl layer consists of two-dimensional successive linkages of the FeO_4Cl_2 octahedral unit as shown in Figure 1b, it is only the five interatomic distances of Fe−O(1), Fe−O(2), Fe−Cl, Fe···Fe(a), and Fe···Fe(b) that should be independently determined,[29] even in the case of fitting over long distances. Determining these five independent distances is, along with the space group information, knowledge of the special positions the atoms lie on, and the unit cell parameters, sufficient to completely determine the structure. The first step was performed by considering all the SS paths within about 6 Å except for the contribution of oxygen atoms that are not directly bonded to the central iron atom because of their weak backscattering power. In the next step, three- or four-body multiple scatterings (DS and TS) with bond angles larger than 150°, which correspond to Fe−O(1)−Fe(a), Fe−O(1)−Fe(4), and Fe−Fe(b)−Fe(5), were included. By considering the MS paths, a better fit could be achieved when only SS paths were considered. The fitted spectra of $k^3\chi(k)$ and FT are shown in Figure 7, together with the experimental spectra, and the $k^3\chi$-(k)s corresponding to individual paths are presented in Figure 8. The structural parameters obtained from the fit are presented in Table 2 together with the crystallographic data from the literature.[22] The distances to the first neighboring atoms and the second neighboring iron atoms are consistent with the crystallographic values to within 0.02 Å.

The analyses of EXAFS data for the alkoxy substituents have been performed only for the methoxy substituent since it was determined to be single phase according to powder X-diffraction analysis and to have the highest substitution ratio. The EXAFS fit was carried out with the theoretical amplitude and phase function calculated assuming the oxygen atoms occupy completely the chlorine sites of the unit cell of FeOCl. The other fitting conditions were almost the same in the case of FeOCl. Even though some stacking faults may lead to a disorder of the crystal structure of the methoxy substituent, the space group may not be largely changed from *Pmmn* of FeOCl, considering the size and shape of the methoxide. This space group, *Pmmn*, is a good place to start in describing the structure of the layers. The obtained structural parameters were used to determine the new a- and b-cell parameters and fractional coordinates in the

(29) In the MOCl system having space group *Pmmn*, there are three independent atomic positions of Fe, O, and Cl atoms (see Table 4), and the other unknown values are the cell parameters a, b, and c. During curve fitting, we should, therefore, seek the bond lengths, Fe−O(1), Fe−O(2), Fe−Cl, Fe···Fe(a), and Fe···Fe(b), constraining to the space group *Pmmn*. However, we used the crystallographic value of 7.92 Å as the Fe···Fe(c) distance out of the fitting range.

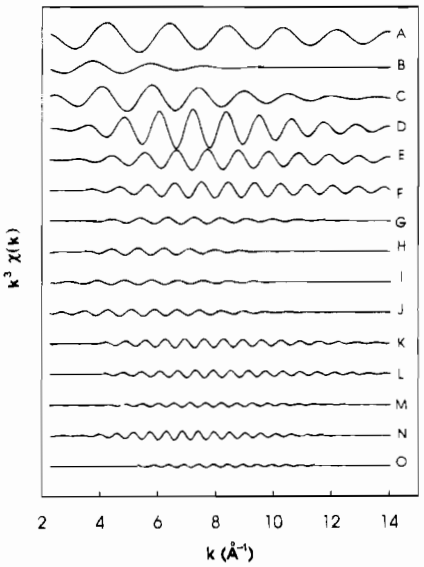

Figure 8. EXAFS signals for individual paths that were included in the best fit for FeOCl: (A) Fe−O(1); (B) Fe−O(2); (C) Fe−Cl(1); (D) Fe−Fe(1); (E) Fe−Fe(*b*); (F) Fe−Fe(*a*); (G) DS Fe−O(1)−Fe(*a*); (H) TS Fe−O(1)−Fe(*a*); (I) Fe−Cl(2); (J) Fe−Cl(3); (K) Fe−Fe(2); (L) Fe−Fe(3); (M) Fe−Fe(4); (N) DS Fe−O(1)−Fe(4); (O) TS Fe−Fe(*b*)−Fe(5).

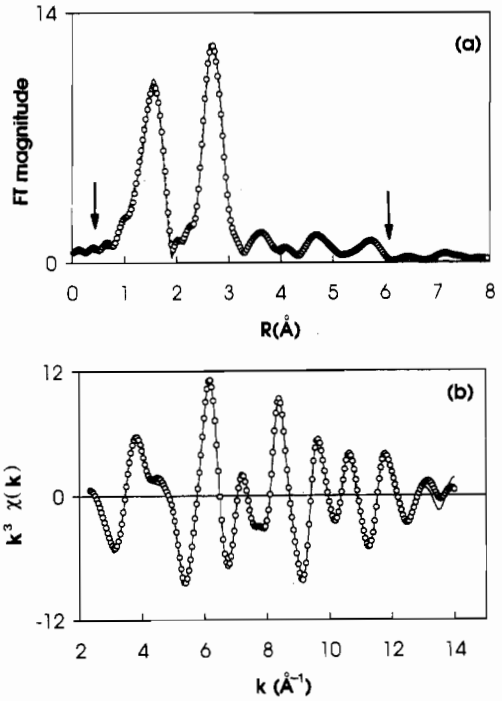

Figure 9. Comparison of the fitted spectra (−) with the experimental data (O) for $FeOCl_{0.13}(OCH_3)_{0.87}$ in *R* (a) and *k* (b) spaces. The range over which the fit has been made is shown by the arrows.

Pmmn space group. The curve fitting was carried out again, using backscattering amplitude and phase shift functions recalculated on the basis of the modified structural data. This analytical procedure was repeated until the fitting results became self-consistent. In the curve fitting, the contributions of carbon and hydrogen atoms were not included, and the coordination numbers of methoxy-oxygen ($O_{methoxy}$) and chlorine atoms were fixed at 1.74 and 0.26, respectively, according to the substitution ratio determined by the elemental analysis. Without any consideration of the chlorine atom, the small peak at 2 Å of the FT could not be well simulated. The fitting results for $k^3\chi(k)$ and FT are compared to the experimental results in Figure 9, and $k^3\chi(k)$s of the individual paths are plotted in Figure 10. The

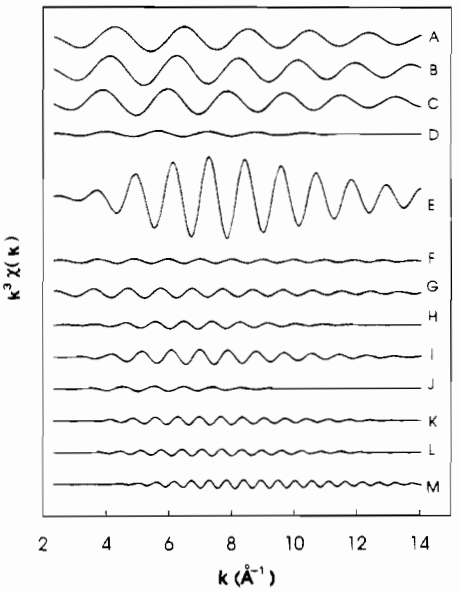

Figure 10. EXAFS signals for individual paths that were included in the best fit for $FeOCl_{0.13}(OCH_3)_{0.87}$: (A) Fe−$O_{methoxy}$; (B) Fe−O(1); (C) Fe−O(2); (D) Fe−Cl(1); (E) Fe−Fe(1 and *b*); (F) Fe−O(3); (G) Fe−O(4); (H) Fe−Fe(*a*); (I) Fe−Fe(2); (J) Fe−Fe(3); (K) DS Fe−O(1)−Fe(*a*); (L) TS Fe−O(1)−Fe(*a*); (M) TS Fe−Fe(*b*)−Fe(5).

Table 4. Unit Cell Parameters and Fractional Atomic Coordinates Estimated from Bond Distances Determined by the Analysis of EXAFS Data for $FeOCl_{0.13}(OCH_3)_{0.87}$[b]

atom	site	*x*	*y*	*z*
Space Group = *Pmmn* with Unit Cell Parameters of $a = 3.89_0$, $b = 3.09_0$, and c[a] $= 10.00_5$ Å				
Fe	2*b*	0.25	0.75	0.091_9
$O_{lattice}$	2*a*	0.75	0.75	0.043_7
$O_{methoxy}$	2*a*	0.75	0.75	0.793_0
CH_3	2*a*	0.75	0.75	0.662_0[a]
Cl	2*a*	0.75	0.75	0.724_0

[a] These values are obtained from powder X-ray diffraction analysis. [b] Occupancy factor is 0.87 for $O_{methoxy}$ and CH_3 and 0.13 for Cl.

fitted structural parameters are represented in Table 3. As is already expected qualitatively from the XANES spectra, the Fe−O bond distances in $FeOCl_{0.13}(OCH_3)_{0.87}$ become similar to one another, resulting in a more regular octahedral symmetry around the iron compared to that in FeOCl. In addition, it is confirmed that the Fe···Fe(*b*) bond distance becomes equal to the nearest Fe···Fe(1) bond distance at 3.09 Å, which is normally observed in iron oxides[28] and alkoxide complexes[30] with an edge-shared octahedral linkage.

In Table 4, the unit cell parameters and the fractional atomic coordinates for the present methoxy substituent were calculated on the basis of the Fe K-edge EXAFS analysis and *Pmmn* space group. It was clearly found that the unit cell parameters of the *a*- and *b*-axis are very similar to those (a = 3.87 Å and b = 3.06 Å) for γ-FeOOH.

Figure 11 shows one-dimensional electron-density maps along the *c*-axis of the FeOCl and methoxy substituent, respectively. In the case of the methoxy substituent, the signs of the structure factors were at first determined by using fractional coordinates of Fe, $O_{lattice}$, $O_{methoxy}$, and Cl atoms, which were obtained from the EXAFS fitting results (Table 4), and recalculated to include the contribution due to the carbon atom at 1.43 Å from

(30) (a) Thich, J. A.; Ou, C. C.; Powers, D.; Vasiliou, B.; Mastropaolo, D.; Potenza, J. A.; Schugar, H. J. *J. Am. Chem. Soc.* **1976**, *98*, 1425. (b) Chiari, B.; Piovesana, O.; Tarantelli, T.; Zanazzi, P. F. *Inorg. Chem.* **1984**, *23*, 3398. (c) Estes, E. D.; Scaringe, R. P.; Hatfield, W. E.; Hodgoson, D. J. *Inorg. Chem.* **1977**, *16*, 1605.

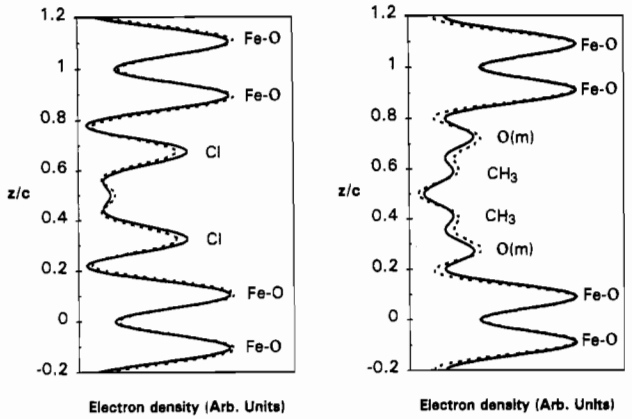

Figure 11. One-dimensional electron-density mappings along the *c*-axes of FeOCl (left) and $FeOCl_{0.13}(OCH_3)_{0.87}$ (right). The dotted and solid lines are calculated on the basis of the intensities of the (00*l*) reflections to seventh order of the powder XRD patterns and structural parameters obtained by EXAFS analyses, respectively.

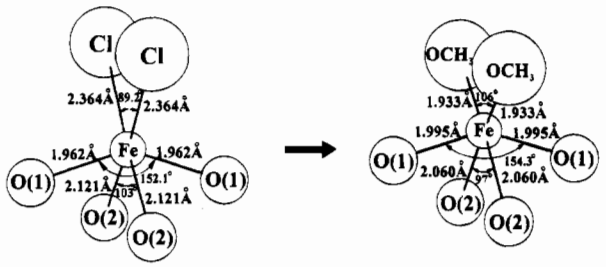

Figure 12. Change of local structure around the iron for FeOCl (left) and its $FeOCl_{0.13}(OCH_3)_{0.87}$ (right) obtained from the analyses of Fe K-edge EXAFS spectra. It can be seen that the local crystal symmetry at the iron site becomes higher upon the substitution reaction.

$O_{methoxy}$.[31] The relative position of the carbon atom was determined by optimizing the residual sum of squares between the electron densities calculated from EXAFS fitting parameters and calculated from the observed XRD intensities. Considering the resultant carbon position (0.662) along the *c*-axis, the distance from $O_{methoxy}$ to CH_3 along the *c*-axis is 1.31 Å, which is shorter than the expected (C−O) bond distance of 1.43 Å. This short distance may be due to a slight tilting of the CH_3 group with respect to the perpendicular plane of $Fe-O_{lattice}$ double layers[6] or due to the sp^2 hybrid character of $O_{methoxy}$.[30c] By comparison of the electron-density map for FeOCl to that for its methoxy substituent, the Fe−O double layers are nearly unchanged, but the peak around $z/c = 0.3$ is moderately diminished in the methoxy substituent as the chlorine atoms are replaced by methoxide having lower scattering power. One-dimensional electron-density maps obtained from the observed X-ray diffraction intensities are consistent with those calculated on the basis of the structural parameters in Table 4, which confirms the reliability of our EXAFS results.

Figure 12 shows how the local symmetry around the iron changes upon the topochemical substitution of chloride ion by the methoxy group. Three different bond distances within the octahedron become similar to one another upon substitution. Furthermore, the bond angle Cl−Fe−Cl of 89.2° in FeOCl increases to 106° ($CH_3O-Fe-OCH_3$) in the methoxy derivative. Such a bond angle is often observed in many alkoxide- and hydroxide-bridged compounds.[30] The bond angles of O(1)−Fe−O(1) and O(2)−Fe−O(2) change from 152° to 154° and from 103° to 97°, respectively (Figure 12). These changes indicate that the local structure around the central iron atom of the substituents is more symmetric than that of FeOCl, as expected from the above Fe K-edge XANES study. These results are also in excellent agreement with the previous prediction from the Mössbauer spectroscopic study[6] but entirely disagree with the previous interpretations[6,8,10] based on the powder X-ray diffraction analysis.

Conclusion

In this work, we show quantitatively how the crystal structure of FeOCl changes upon the topochemical substitution reaction of the chlorine atom by the alkoxy group by means of X-ray absorption spectroscopy at the Fe K-edge. The comparison of XANES spectra for all compounds has shown that the octahedral symmetries around Fe^{III} for alkoxy substituents become more regular than that for FeOCl. To understand the detailed crystal structures, analyses of EXAFS data at Fe K-edge were carried out for FeOCl and its methoxy substituent. The fitted bond distances for FeOCl are in good agreement with the previous crystallographic data, which confirms the validity of the present analytic procedure. In the methoxy substituent, each Fe^{III} not only forms a more regular oxygen octahedron with bond distances of 1.93, 2.00, and 2.06 Å but also has a reduced bond length of 3.09 Å with the Fe(*b*) atom along the *b*-axis, resulting in the same distance as the nearest Fe(1) atom. Assuming that the methoxy substituent would have the same space group of *Pmmn* as FeOCl, the fractional atomic coordinates of the methoxy substituent could be estimated from bond lengths determined by the EXAFS data analysis. The reliability of the EXAFS fits is also confirmed by one-dimensional maps calculated from powder X-ray diffraction intensities. Consequently, it is proposed that the crystal structure of the methoxy substituent is nearly the same as that of γ-FeOOH.

Moreover, the present structural model for the methoxy substituent of FeOCl explicitly clears up some questions about the structure proposed by the powder X-ray diffraction method that many researchers have not readily understood up to date. We have successfully proved that our analytical method could be effectively applied to various two-dimensional systems such as MOCl or other layered compounds and their organic derivatives with very poor crystallinity.

Acknowledgment. The present study was supported by the Basic Science Research Institute Program, Ministry of Education (Grant No. BSRI-95-3413), and also in part by the Electronics and Telecommunication Research Institute 1995. We thank the Photon Factory, National Laboratory for High Energy Physics, and the Pohang Light Source for supporting the synchrotron radiation experiments. Our thanks are extended to Professor M. Nomura for his help in obtaining X-ray absorption data at the beam line BL10B.

Supporting Information Available: Figures 1S and 2S showing powder XRD patterns for methoxy and ethoxy substituents, respectively (2 pages). Ordering information is given on any current masthead page.

(31) Venkateswarlu, P.; Gordy, W. *J. Chem. Phys.* **1955**, *23*, 1200.

IC950755K